Tellus SERIES B CHEMICAL AND PHYSICAL METEOROLOGY
PUBLISHED BY THE INTERNATIONAL METEOROLOGICAL INSTITUTE IN STOCKHOLM

Tellus (2011), 63B, 309–327
Printed in Singapore. All rights reserved

TELLUS

Monthly, global emissions of carbon dioxide from fossil fuel consumption

By R. J. ANDRES[1]*, J. S. GREGG[2], L. LOSEY[3], G. MARLAND[1] and T. A. BODEN[1],
[1]*Environmental Sciences Division, Oak Ridge National Laboratory, Oak Ridge, TN 37831-6290, USA;* [2]*Risø DTU National Laboratory for Sustainable Energy, 4000 Roskilde, Denmark;* [3]*Department of Space Studies, University of North Dakota, Grand Forks, ND 58202-9008, USA*

(Manuscript received 21 June 2010; in final form 16 February 2011)

ABSTRACT

This paper examines available data, develops a strategy and presents a monthly, global time series of fossil-fuel carbon dioxide emissions for the years 1950–2006. This monthly time series was constructed from detailed study of monthly data from the 21 countries that account for approximately 80% of global total emissions. These data were then used in a Monte Carlo approach to proxy for all remaining countries. The proportional-proxy methodology estimates by fuel group the fraction of annual emissions emitted in each country and month. Emissions from solid, liquid and gas fuels are explicitly modelled by the proportional-proxy method. The primary conclusion from this study is the global monthly time series is statistically significantly different from a uniform distribution throughout the year. Uncertainty analysis of the data presented show that the proportional-proxy method used faithfully reproduces monthly patterns in the data and the global monthly pattern of emissions is relatively insensitive to the exact proxy assignments used. The data and results presented here should lead to a better understanding of global and regional carbon cycles, especially when the mass data are combined with the stable carbon isotope data in atmospheric transport models.

1. Introduction

Carbon dioxide (CO_2) released to the atmosphere from the combustion of fossil fuels is a major contributor, and the major anthropogenic contributor, to the rise of the CO_2 concentration observed in the atmosphere (91% of the 9.28 Pg C released to the atmosphere in 2009, Le Quere et al., 2009). This relationship between emissions and concentration is directly supported by at least five lines of evidence: (1) the temporal correlation between quantities emitted and concentrations observed (Forster et al., 2007), (2) the North–South gradient of atmospheric CO_2 concentration (Denman et al., 2007), (3) the evolution of the atmospheric signature of stable carbon isotopes ($\delta^{13}C$, Ciais et al., 1995), (4) observed changes in the atmospheric signature of radiogenic carbon ($\Delta^{14}C$, Levin et al., 2010) and (5) observed changes in atmospheric oxygen concentration (Keeling et al., 1993). Despite the demonstrated linkage of fossil-fuel emissions and atmospheric concentration, it is difficult to understand the full details of the global carbon cycle because of the large temporal and spatial variability in both the carbon reservoirs (e.g. the biosphere, atmosphere and ocean) and the fluxes between reservoirs (e.g. Le Quere et al., 2009).

The five lines of evidence cited earlier all rely on inventories of fossil-fuel CO_2 ($FFCO_2$) emissions—so-called 'bottom-up' inventories. Although national $FFCO_2$ inventories are now being compiled by many countries, largely in response to the United Nations Framework Convention on Climate Change (United Nations, 1992) and its Kyoto Protocol (United Nations, 1998), via the Intergovernmental Panel on Climate Change (IPCC) guidelines (IPCC, 2006), global and some national $FFCO_2$ inventories have been compiled for much longer time periods. These national inventories rely on energy data assembled by the individual countries while the global inventories rely on energy production, trade and consumption data compiled by the United Nations (e.g. United Nations, 2008), the International Energy Agency (e.g. International Energy Agency, 2009), the United States Department of Energy (EIA, 2010) or on other archived statistics (e.g. Etemad et al., 1991; BP, 2009). The longest and most complete of these global inventories contains annual $FFCO_2$ emissions estimates, by country, from 1751 to the present (Marland and Rotty, 1984; Andres et al., 1999; Boden et al., 2009). The Carbon Dioxide Information Analysis Center (CDIAC) data used in this study compare to other global inventories to within 5% (Macknick, 2009).

*Corresponding author:
e-mail: andresrj@ornl.gov
DOI: 10.1111/j.1600-0889.2011.00530.x

All of the emissions inventories mentioned earlier, and the five lines of evidence listed for linking emissions and concentration, are based on inventories that are national or global in spatial scale and annual in temporal scale. With increasing concern about the climate impacts of increasing atmospheric CO_2 has come increased interest in the details of the global carbon cycle, increased interest in the details of responsibility for CO_2 emissions, and increased interest in trying to limit or otherwise control emissions. All of these lead to a need for emissions inventories that have finer resolution than national and annual scales. In response to this need, the International Energy Agency and many countries are now producing inventories that have sectoral details. Andres et al. (1996) and EDGAR (http://edgar.jrc.it; Olivier et al., 2005) have produced global inventories on a spatial grid, the European Union Greenhouse Gas Emission Trading System (EU, 2009) and similar initiatives elsewhere have stimulated inventories at the corporate, plant or city level (e.g. NYC, 2010), and tools are available for businesses and households to estimate their emissions inventories. The Vulcan Project has produced for the United States an emissions inventory at 10 km scale for the year 2002 (Gurney et al., 2009) and initiatives in Germany (Pregger et al., 2007) have produced similar inventories for Europe. Oda and Maksyutov (2011) and Rayner et al. (2010) have started to examine the use of night light imagery to improve spatial resolution of emission estimates. The various initiatives to improve spatial and temporal resolution have different objectives, different data needs, and are adopting different approaches because data on fossil-fuel combustion are universally available only at national and annual scales, and even at national and annual scales there are problems [e.g. inconsistent state-level and national-level totals, data transcription errors, proper gas flaring accounting, reporting fuel use in non-fuel use applications (e.g. plastic feedstocks, . . .)] and missing data.

It is also now becoming apparent that international efforts to limit CO_2 emissions or to trade emission permits will likely require some approach to monitoring and verification of emissions inventories. This is necessary to assure that countries are meeting their commitments and that those who buy emissions permits or emissions offsets are indeed receiving what they purchased. Although self-reported emissions inventories can serve many purposes, some independent verification (e.g. a potential for falsification) of these inventories can be supplied with atmospheric or remotely sensed data. Corroboration of atmospheric and remotely sensed data (top down) with self-reported inventories (bottom up) will be facilitated if the spatial and temporal resolutions of these bottom up inventories are improved (see, e.g. IPCC, 2010; NRC, 2010). Recent analyses show that the highest priority for improving the utility of emissions inventories for atmospheric modelling is to improve representation of the annual cycle of emissions (Gurney et al., 2005; Corbin et al., 2010).

There is thus both scientific and public policy motivation for improving both the spatial and temporal resolution of $FFCO_2$ inventories. This paper summarizes the data available, describes the development of a data set and presents a description of monthly, global, $FFCO_2$ emissions from 1950 to 2006. Data are presented in terms of the mass of emissions, their latitudinal and longitudinal distribution, and their $\delta^{13}C$ signatures. These estimates are based on the finest-resolution data on energy consumption that are available over a significant fraction of global $FFCO_2$ consumption. Still, considerable extrapolation and data processing have been necessary to arrive at estimates of global, monthly $FFCO_2$ emissions.

2. Methodology and data used

Although international energy statistics are generally compiled at the level of countries and years, some countries do compile some data on energy consumption at the level of months, and some larger countries compile such data at the level of states or provinces. The focus here is on describing the annual cycle of emissions and is thus on monthly data. To estimate emissions at finer temporal scales may require modelling the temporal variability of energy consumption (e.g. Vulcan). For a given country, monthly data are often available for only some fuel commodities, some fuel-use sectors and/or for some limited time interval. The focus here is using publicly available data to approximate the global and regional emissions of $FFCO_2$ emissions on a monthly basis. The work presented here builds on monthly national/regional studies already published for The United States (Gregg and Andres, 2008), China (Gregg et al., 2008), Brazil (Losey et al., 2006) and North America (Gregg et al., 2009). The approach for using data that are available to approximate the distribution where complete data are not available is described in Gregg and Andres (2008).

The monthly, global, $FFCO_2$ emissions data set presented here is the result of a proportional-proxy method. The method has five basic steps: (1) compile available data on the monthly fossil fuel consumption in each country; (2) calculate the fraction of fuel consumed in each month in each country for each fuel; (3) pair all countries with a proxy country that has known monthly data; (4) for country-year pairs with no monthly data, determine monthly fractions via proxy assignments and Monte Carlo methods and (5) calculate monthly $FFCO_2$ emissions by multiplying monthly fractions by annual $FFCO_2$ emission estimates. The method is proportional because for the 21 countries listed in Table 1, the proportional methodology presented in Gregg and Andres (2008) was used to determine monthly national emissions. This methodology parses the annual $FFCO_2$ emissions into monthly emissions by using the available monthly data for each country. The method is proxy because the monthly patterns observed in these 21 countries were used as surrogates for years and countries where monthly data are lacking. The proxy methodology is the primary new methodology presented in this paper.

Table 1. Ranking of countries according to total $FFCO_2$ emissions for 2006

Rank	Country	Emissions	
		Mass (Tg C)	Cumulative (%)
1	China (mainland)	1665	21
2	United States of America	1569	41
3	Russian Federation	427	47
4	India	412	52
5	Japan	353	57
6	Germany	220	59
7	United Kingdom	155	61
8	Canada	149	63
9	Republic of Korea	130	65
10	Italy (including San Marino)	129	67
11	Islamic Republic of Iran	127	68
12	Mexico	119	70
13	South Africa	113	71
14	France (including Monaco)	104	72
15	Saudi Arabia	104	74
16	Australia	101	75
17	Brazil	96	76
18	Spain	96	78
19	Indonesia	91	79
20	Ukraine	87	80
21	Poland	87	81
All	Total for all 212 countries	7828	100

Table adapted from CDIAC data reported in Boden et al. (2009).

2.1. Proportional methodology

The countries specifically listed in Table 1 were the largest mass $FFCO_2$ emitting countries in the world as of 2006 (the latest available data when this paper was being written). The 1998 list (not shown) contains the same countries, but in a different order. The year 1998 was the most recent year for which data were available when the task of searching for and evaluating monthly data commenced. The countries on both lists collectively accounted for 80% of global $FFCO_2$ emissions. Table 1 emphasizes that the majority of emissions are dominated by a small number of countries. Because of their vast majority proportion of the global total, these countries largely define the global pattern of $FFCO_2$ emissions.

Figure 1 shows the countries, fuels and years for which significant monthly data were located. The time series are of different lengths because the underlying statistics used for the proportional methodology began and ended at different times for different countries and even for different fuels within one country. Some of the underlying statistics are now available online but many others are not and involved a time-consuming process of making/maintaining personal contacts and even of travelling to national and international statistical agencies to get data. See Appendix S1 for the data sources used. This listing of sources is given so that future users of this data can easily identify the underlying data used to make the monthly time series and thus extend the time series if they desire.

The result of the data collection described earlier is 62 separate time series of monthly fractions for solid, liquid and gaseous fuels (individually) covering the 21 countries. These monthly fractions represent the proportion of solid, liquid or gaseous fuel consumed in each month of a given year and their sum over a given year equals 1.000. Thus, monthly emissions for a given country and fuel could be calculated by multiplying the monthly fractions by the well-accepted CDIAC solid, liquid or gaseous $FFCO_2$ emission estimates for the same country, fuel and year (Boden et al., 2009). The use of monthly fractions makes individual solid, liquid and gas totals consistent with the CDIAC-reported annual, national totals. Figure 2 compares the relationship between the data with a known monthly distribution (i.e. for the 21 chosen countries) and the data with an unknown monthly distribution (i.e. the remaining countries) for the years 1950–2006. As seen in Fig. 1, for years 1956–1970, monthly data are available for only Australian coal, but at its peak, the data for the known countries and fuels explicitly account for 77% of total global $FFCO_2$ emissions (Fig. 2); thus, leaving only 23% to be inferred by the proportional-proxy method for that year.

2.2. Proxy methodology

After completion of the proportional methodology for 21 countries, a mapping table was constructed to complete the proxy methodology. This table mapped the monthly fraction patterns for all countries by assigning each country without monthly data to a proxy based on one country of the 21-country sample with monthly data. The mapping was based upon similarities in climates and economies. Climate similarities included grouping countries into northern, equatorial or southern latitudes so that the phasing of winter/summer would be correct. Economic similarities included considerations such as capitalistic versus centrally planned economies. For the few countries where these two considerations were insufficient to determine the proxy country, geographic closeness was used to determine the proxy country. See Appendix S2 for the mapping table. Although one could quibble over exact proxy assignments, as discussed in Sections 4.2 and 4.3, these assignments have little effect on the global $FFCO_2$ emission pattern. For example, although Indonesia contributes 1% of global $FFCO_2$ emissions (Table 1), it is the proxy for 44 additional countries on three continents. These 44 countries contribute less than 2% of global $FFCO_2$ emissions. Thus, although the absolute number of countries is large, its relative effect on emissions is small.

With completion of the proportional methodology for 21 countries and completion of the mapping table, a global $FFCO_2$ emissions monthly time series could be completed. Monte Carlo simulations were used to apply monthly fractions from fuels and

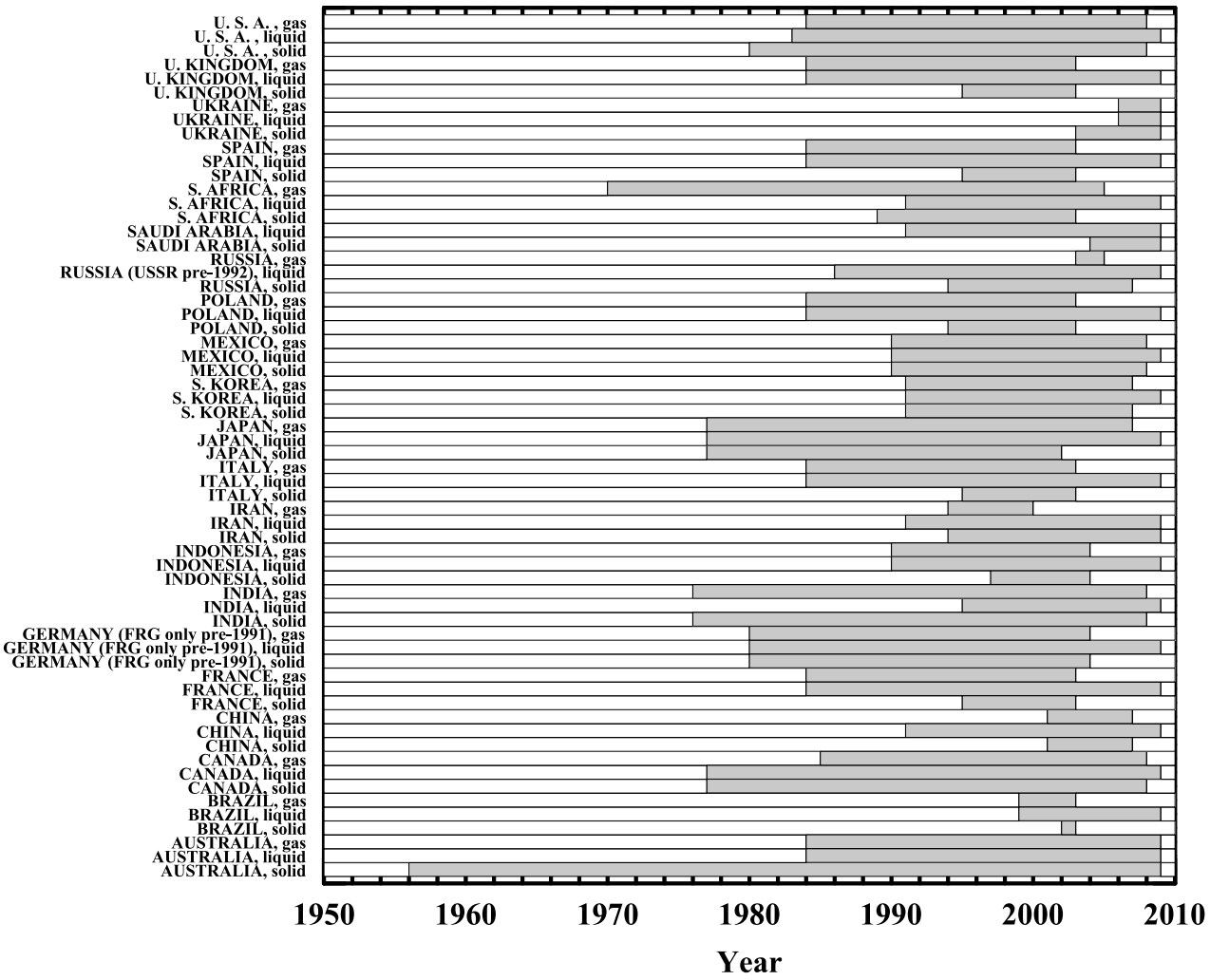

Fig. 1. Grey bands indicate the 21 countries, fuels and years for which monthly data exist. The annual jumps in the curves that occur in Fig. 2 are partially due to the existence of monthly data.

years with monthly data to the same fuel and additional years without monthly data. As a within-country example, for solid fuels in India (one of the 21 countries), a randomly selected solid-fuel monthly fraction pattern from one of the 32 known India solid-fuel annual patterns (years 1976–2007 inclusive) was applied to the year 1950 solid fuels and another randomly selected solid-fuel monthly fraction pattern was selected for each of the remaining years without explicit solid-fuel monthly data. As a cross-country example, for liquid fuels in Pakistan (not one of the 21 countries, but mapped to the India monthly patterns), a randomly selected liquid-fuel monthly fraction pattern from one of the seven known India liquid-fuel annual patterns (years 1995–2001 inclusive) was applied to the year 1950 liquid fuels and another randomly selected liquid-fuel monthly fraction pattern was selected for each of the remaining years without explicit liquid-fuel monthly data. Note that solid, liquid and gaseous fuels each have a randomly selected monthly fraction pattern selected independently from each other; thus if a 1975 solid fuel monthly fraction pattern is selected to represent the 1955 solid fuel emission pattern, that does not imply that the 1955 liquid fuel emission pattern will be represented by the 1975 liquid fuel monthly fraction pattern.

The use of the Monte Carlo approach preserves a more realistic amplitude for the annual cycle for years and countries in which monthly data are lacking. The use of an average of known monthly data tends to flatten the annual cycle. Thus, the real effect of the Monte Carlo approach is to preserve a more realistic seasonal cycle in each country. Its effect disappears as data are aggregated across space and/or time. For any method chosen to extrapolate from the known monthly data to unknown spatial and temporal domains, it becomes important to distinguish between real trends from those that are imposed through the extrapolation process. Thus, specific local (i.e. national) trends are suspect whereas global trends are more

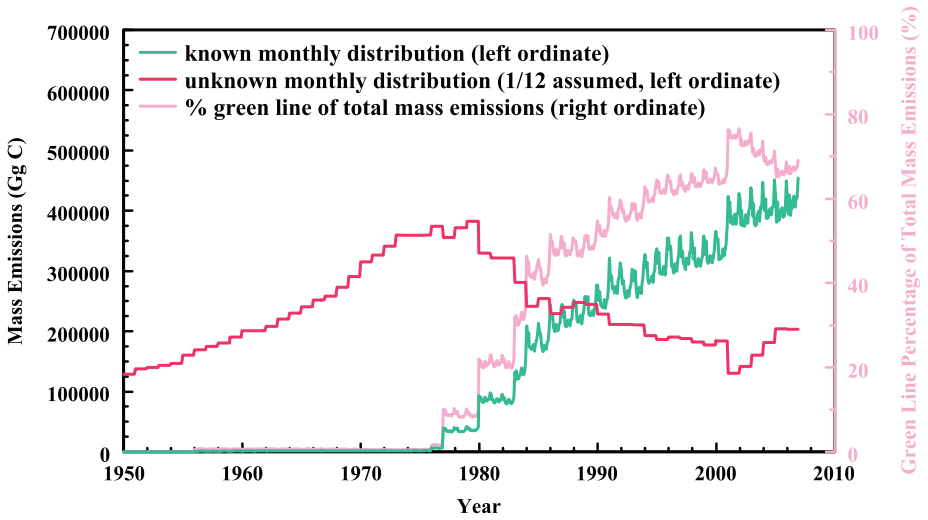

Fig. 2. The mass of global $FFCO_2$ emissions for which there is monthly data versus the mass of global $FFCO_2$ emissions for which there is no monthly data. The data of known monthly distribution show the annual cycle of emissions. The data of unknown monthly distribution appear in flat monotonic steps because emissions are assumed in this plot to be uniform over the year (equal to 1/12 of the annual total in each month). Data of known monthly distribution were calculated separately for solid, liquid and gaseous fuels. The sum of those three fuels is displayed in this graph. Note that emissions from gas flaring and cement are not included in this graph as monthly data for these two categories are limited to only a few countries. The pink line was calculated from the mass of emissions represented by the green line divided by the sum of the mass of emissions represented by the green and red lines.

robust due to statistical averaging processes. Uncertainties associated with this Monte Carlo approach are addressed later in this paper.

2.3. $FFCO_2$ *emissions from gas flaring and cement*

Finally, the complete CDIAC $FFCO_2$ emissions time series contains emissions from gas flaring and cement production (e.g. Boden et al., 2009). At this time, these two categories which compose 2–5% of the global total do not have reliable monthly statistics with which to subdivide their emissions into monthly fractions for most countries of the world. Thus, the monthly, global, $FFCO_2$ time series presented here contains these emissions, but they are distributed uniformly throughout the year (Fig. 3). This 1/12 distribution does not change the shape of the monthly curve when the curve is examined in annual increments. However, this 1/12 distribution does offset the curve up or down depending on the magnitude of the gas flaring plus cement emissions. The inclusion of gas flaring and cement production makes the national and global totals presented here directly comparable to and consistent with the CDIAC-reported national and global annual totals.

2.4. *Mass spatial distributions*

With estimates of $FFCO_2$ emissions by month for all countries it is possible to derive estimates of the spatial distribution of emissions by month. Figures 4 and 5 show, for example, the latitudinal (Fig. 4) and longitudinal (Fig. 5) distribution of emissions in December and the data set permits similar constructs for all other months. These distributions are based on the 1 degree $\times$ 1 degree latitude–longitude distribution described by Andres et al. (1996) and on a within-country distribution based on population density. Figures 4 and 5 are from a single Monte Carlo simulation as described earlier. Other $FFCO_2$ distribution methodologies exist in the literature. Each methodology has its own strengths and weaknesses.

2.5. *Stable carbon isotope spatial distributions*

With estimates of $FFCO_2$ emissions by month and fuel for all countries it is also possible to derive estimates of the stable carbon isotope signature of emissions by month using the stable carbon isotope signatures presented in Andres et al. (2000). The signatures presented here are mass-weighted, reflecting the amount of a particular fuel consumed multiplied by its signature. These mass-weighted signatures can help differentiate $FFCO_2$ processes from biologic and oceanic processes. Figure 6 shows the time series of $\delta^{13}C$ for global $FFCO_2$ emissions by month. These emissions can be distributed spatially as done for the mass of emissions earlier. Figures 7 and 8 show, for example, the latitudinal (Fig. 7) and longitudinal (Fig. 8) signature of emissions in December and the data set permits similar constructs for all other months.

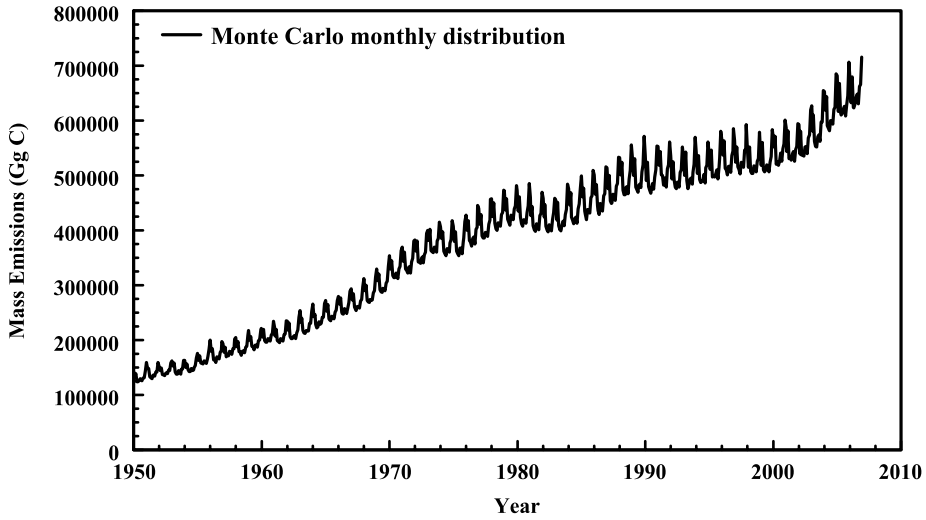

Fig. 3. The monthly distribution of the mass of global $FFCO_2$ emissions based on one Monte Carlo simulation. The curve shown represents the $FFCO_2$ emissions from solid fuels, liquid fuels, gas fuels, gas flaring and cement production.

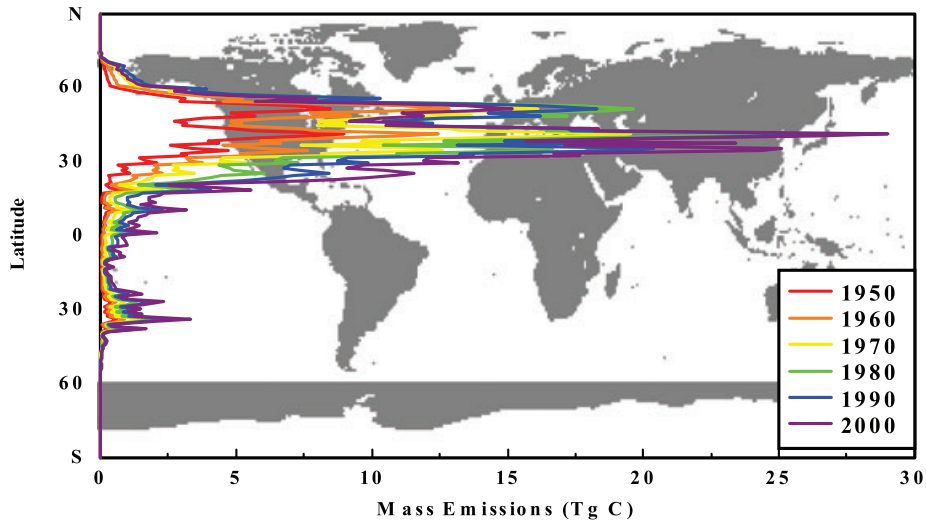

Fig. 4. Latitudinal profiles of December $FFCO_2$ emissions at 10-year time intervals. The December emissions are illustrated here, but data exist for all months. In the background is a one-degree map of the world so the emission curves can be matched to geography. The grey band around Antarctica is the Antarctic Fisheries.

3. Results and discussion

3.1. Mass results and discussion

3.1.1. Two basic results. Figure 3 shows two major attributes of the monthly emissions time series that are of particular interest here. The first attribute is the general increase with time of $FFCO_2$ emissions. This is in accord with the annual data that form the foundation of the monthly data.

The second attribute observed in Fig. 3 is the apparent growth in the amplitude of the annual cycle with time, where the amplitude of the annual cycle is defined as the difference between the maximum and minimum monthly emission estimates in any given year. Figure 9 explicitly shows growth in the amplitude of the annual cycle over the 56 years of the time series.

3.1.2. Is growth in seasonal cycle real or an artefact? The growth in amplitude of the annual cycle could be explained as the result of a changing mix of $FFCO_2$ emissions from various countries with different annual patterns. Figure 4 shows that the latitudinal distribution of $FFCO_2$ emissions is changing with time, including the ratio of Northern Hemisphere and Southern Hemisphere emissions which tend to peak about one half year apart. This increase in emissions coupled with a changing mix of emissions from various countries could contribute to annual cycle amplitude growth.

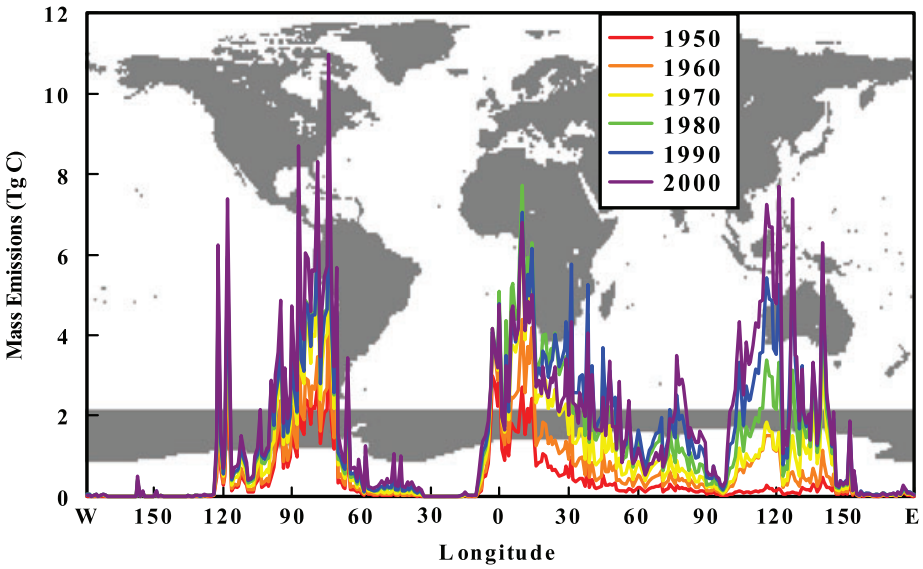

Fig. 5. Longitudinal profiles of December $FFCO_2$ emissions at 10-year time intervals. The December emissions are illustrated here, but data exist for all months. In the background is a one-degree map of the world so the emission curves can be matched to geography.

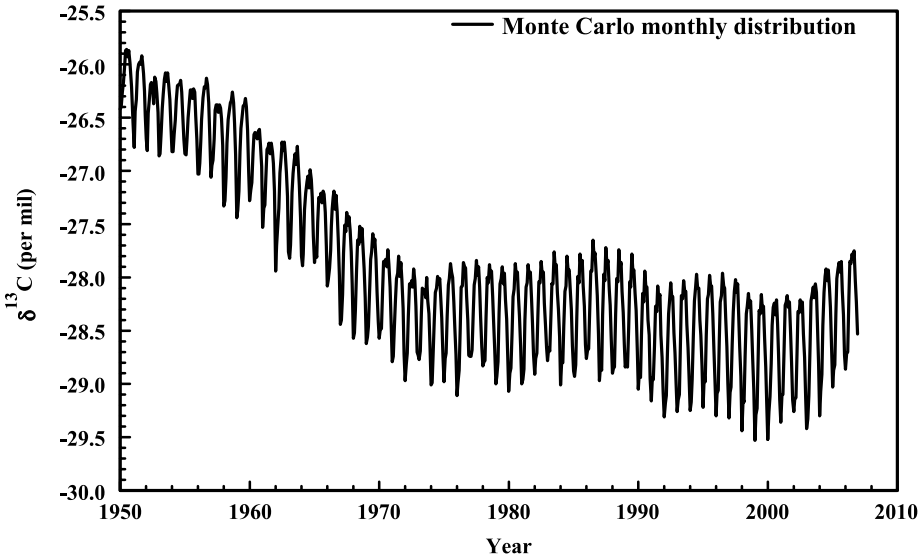

Fig. 6. The monthly distribution of the stable carbon isotopic signature of global $FFCO_2$ emissions based on one Monte Carlo simulation.

Alternatively, the growth in amplitude of the annual cycle could be explained by the basic computational process of using relative monthly proportions in an overall framework of absolute annual emissions growth. This can lead to an annual cycle that grows in absolute amplitude in direct proportion to the magnitude of emissions.

The coefficient of variation statistic, the standard deviation divided by the mean of the monthly emission estimates in a given year, was used to test the relationship between the annual mass of emissions and the amplitude of the annual cycle. This is not a perfect test as the attribute is about the amplitude of the annual cycle determined from minimum and maximum values while the coefficient of variation looks at the bulk of monthly emission values through its use of the standard deviation. However, the coefficient of variation was used because our general interest is in whether the overall shape of the annual cycle is changing with time; this is a property of the bulk of monthly emissions estimates. The minimum and maximum outliers have helped point to this analysis.

Analysis shows that the coefficient of variation slowly declines with time from a value of 0.45 in 1950 to 0.40 in 2006. This indicates that the mean monthly emission estimate is increasing faster than the standard deviation of the monthly emission estimates in a given year. So, although Figs. 3 and 9 show

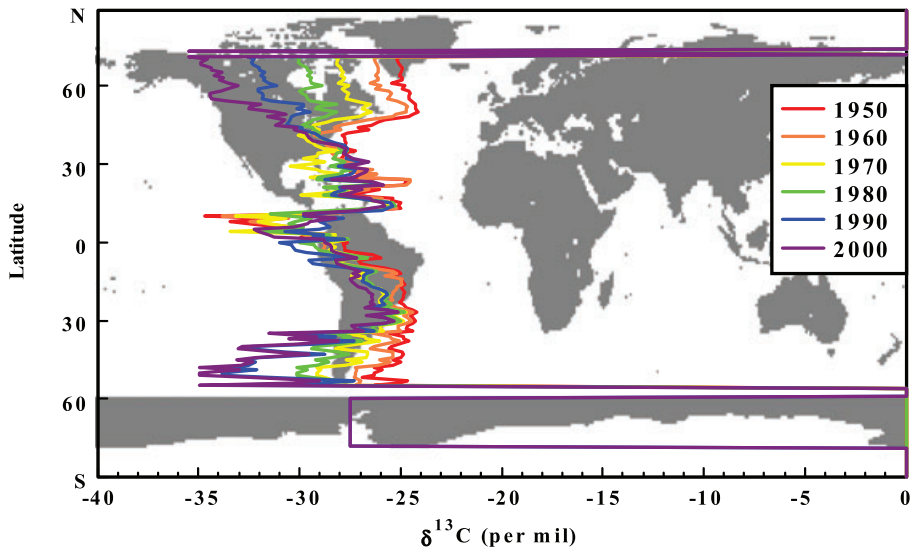

Fig. 7. Latitudinal profiles of December $\delta^{13}C$ of $FFCO_2$ emissions at 10-year time intervals. The December emissions are illustrated here, but data exist for all months. In the background is a one-degree map of the world so the emission curves can be matched to geography. The effects of emissions from the Antarctic Fisheries are seen in the year 2000 in the Southern Ocean. Values of $\delta^{13}C$ shown equal to zero indicate one-degree latitude bands with no emissions or no data (e.g. Antarctic Fisheries in 1980).

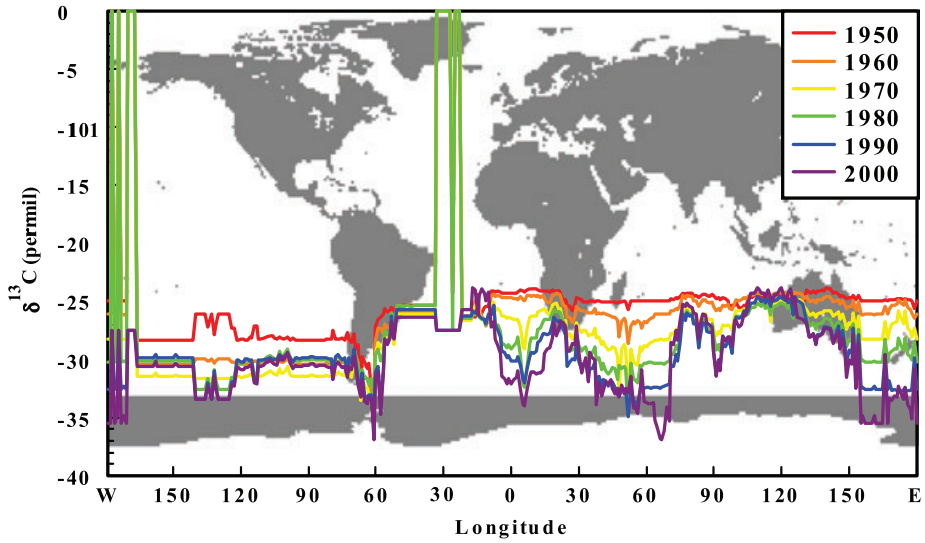

Fig. 8. Longitudinal profiles of December $\delta^{13}C$ of $FFCO_2$ emissions at 10-year time intervals. The December emissions are illustrated here, but data exist for all months. In the background is a one-degree map of the world so the emission curves can be matched to geography. Values of $\delta^{13}C$ shown equal to zero indicate one-degree latitude bands with no emissions or no data (e.g. Antarctic Fisheries in 1980).

an absolute growth in the amplitude of the annual cycle with time, the coefficient of variation and examination of the actual monthly data indicate that this amplitude growth is due to both an overall rise in absolute total emissions and an increase in the month-to-month variability of emissions.

The coefficient of variation analysis and the knowledge that the bulk of $FFCO_2$ emissions occurs in the Northern Hemisphere do not allow us to definitively conclude whether the growth in the amplitude of the annual cycle is an artefact of the Monte Carlo analysis scheme used or is a real property of the actual global $FFCO_2$ emission pattern. Although the coefficient of variation analysis suggests that rising $FFCO_2$ emissions are a factor in the apparent increase in the growth in the amplitude of the annual cycle, it does not directly confirm it quantitatively since it does not directly measure the extremes of the data set. Knowledge that the bulk of $FFCO_2$ emissions occurs in the Northern Hemisphere and that the percentage of emissions in the Northern Hemisphere is increasing with time leads to the conclusion that the extremes

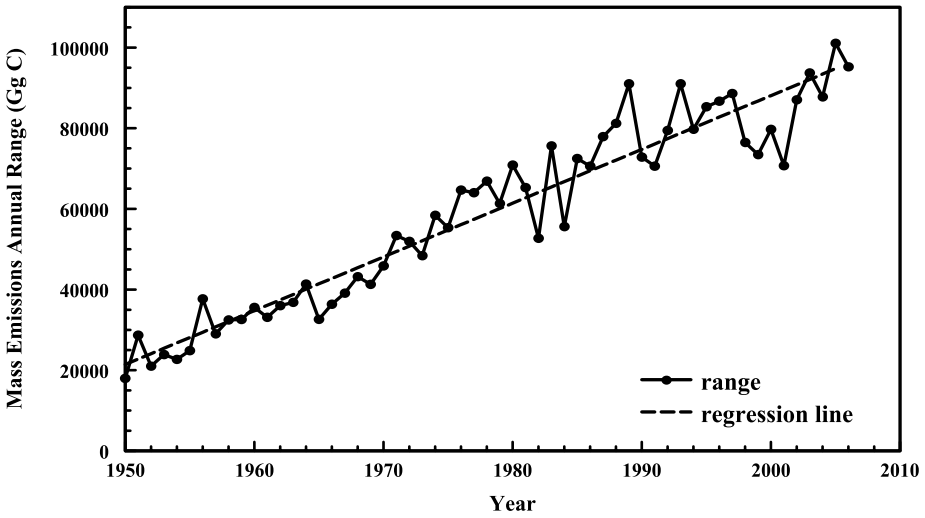

Fig. 9. The annual range in mass of total $FFCO_2$ emissions. The range was calculated from the maximum and minimum monthly values of total $FFCO_2$ emissions for the calendar year. The dashed line is a linear regression through the annual values.

of the global annual cycle are dominantly controlled by Northern Hemisphere emissions. The dilemma, Monte Carlo artefact or real feature, needs further data and analysis to be fully resolved.

3.1.3. Correlation of seasonal cycle shape with fuels. Multiple linear regression analyses of the five individual time series (i.e. solid, liquid, gas, gas flaring and cement) whose sum is represented in Fig. 3 show that the shape of the annual cycle (e.g. January through December in a given year) is most strongly correlated with emissions from solid fuels (especially early in the time series) and with emissions from liquid fuels (especially late in the time series). Gas fuels are the most strongly correlated in only 2 years of the 57 years represented. These correlations are not too surprising as emissions from solid fuels dominate the total emissions early in the time series, but later in the time series emissions from liquid fuels become equal to and in some years surpass those from solid fuels. However, the annual total mass of emissions from a given fuel in a given year does not fully explain these correlations, it is also the distribution of emissions throughout the year which affect the correlations. Different fuels have different annual distributions (e.g. consumption of liquid fuels used for transportation tends to be more uniformly distributed throughout the year than consumption of gas fuels used for heating). These distributions, known from the data represented in Fig. 1, and their proxy representations ultimately shape the curve seen in Fig. 3.

3.1.4. Caution on using specific Monte Carlo results to describe year-specific features. It is also important to note that the Monte Carlo procedure used here can create spurious results for the emission pattern of one country or for the globe if only one particular simulation is analysed. For example, Blasing et al. (2005) and Gregg et al. (2009) show that the shape of the annual cycle in the United States is changing with time; there is a growing secondary maximum in the summer as increased air conditioning requires increased energy consumption. This feature is noticeable because of the monthly detail available for energy consumption in the United States. Thus, for years with unknown monthly consumption patterns, the Monte Carlo simulation may pick a monthly emission pattern from a year with no, emerging, or noticeable summer maximum. The Monte Carlo simulation may also place a noticeable summer maximum in a given year and no summer maximum in the prior year or subsequent year. Although this particular example is limited to affecting the United States only (because the United States serves as a proxy for the United Sates only), the general principle extends to all of the proxy relationships. Particular features in the monthly emission pattern from one of the countries listed in Table 1 will be randomly selected and displayed as a monthly emission pattern in the proxy countries. The result is that multiple year trends in the particular features are not likely to be faithfully portrayed in the time series from the proxy countries. Therefore, when looking for general emission patterns, one needs to average multiple runs of the Monte Carlo simulations to get robust results. The averaging of multiple runs allows random noise to cancel and robust features to be maintained. In general, results from multiple runs are being discussed and displayed in this text, unless specifically noted otherwise.

3.1.5. Are fossil fuel seasonal cycles seen in flask samples from the Earth's atmosphere? Returning to Fig. 9, the amplitude of annual emissions is increasing nearly in a monotonic linear fashion with time. This increase echoes similar results seen in atmospheric flask and in situ atmospheric monitoring networks (e.g. Thoning et al., 1989; Keeling et al., 1996, 2005). Although there are broad similarities between the shapes of the relative annual amplitude curves of Keeling et al. (1996, Fig. 1) and this study (not shown), the growth rates of the curves are dissimilar. Keeling et al. (1996) report growth rates on the

order of 20% at Mauna Loa and 40% in the Arctic for the years 1965–1994. The corresponding growth rate for the data on amplitude of the annual cycle reported here is 140%. Part of this discrepancy can be explained by the fact that only approximately 55% of $FFCO_2$ is ultimately retained in the atmosphere (Scripps data reported in Denman et al., 2007); the rest is absorbed by the biosphere and the oceans. Secondly, $FFCO_2$ is not the only process affecting CO_2 concentrations in the atmosphere; seasonal trends in growth and decay in the biosphere also affect the range of atmospheric CO_2 concentrations (Le Quere et al., 2009). Thus, perfect correspondence between relative amplitude curves of atmospheric CO_2 and $FFCO_2$ is not expected and the annual cycle of CO_2 concentration in the atmosphere is generally attributed to oceanic and biospheric processes. However, Patra (personal communication, 2009) has taken advantage of the monthly $FFCO_2$ data sets presented here to test the hypothesis that monthly changes in $FFCO_2$ emissions can lead to observable changes in atmospheric CO_2 concentrations measured at flask sampling sites. He has completed some preliminary modelling by advecting the monthly $FFCO_2$ emission fields presented here through an atmospheric transport model which included oceanic and biospheric fluxes. His early results indicate there is substantial influence from changes in monthly fossil fuel fluxes on changes in atmospheric flask sample CO_2 concentrations at some atmospheric flask sample sites. This influence is on par with or sometime exceeds influences from biospheric and oceanic fluxes. At other flask sample sites, changes in monthly $FFCO_2$ fluxes do not have such a substantial impact. Kaufmann (personal communication, 2010) has achieved similar results with statistical analyses of time series data of United States monthly emission inventories and atmospheric sampling sites. Further modelling may confirm or deny the importance of the $FFCO_2$ monthly emissions to monthly changes in the atmospheric CO_2 concentration.

3.1.6. Basic attributes of latitudinal and longitudinal distributions. In general, the amplitude of the annual cycle of $FFCO_2$ emissions is higher at high northern latitudes and smaller at low latitudes and high southern latitudes. This is consistent with features seen in earlier studies focused on North America (Gregg et al., 2009) and Brazil (Losey et al., 2006). Table 2 presents some basic attributes of latitudinal profiles of monthly emissions. Table 2 shows that for one degree latitudinal bands, the average amplitude of the annual cycle is relatively small, but (as indicated in Fig. 3) is growing with time. For example, in 2000, there was one latitudinal band in which emissions reached 29.02 Tg C per month with a range of 5.14 Tg C per month (17.72%) between the highest and lowest months. But, on average, the range between highest and lowest months was only 0.78 Tg C (<3%) for one-degree bands which contained $FFCO_2$ emissions. When latitudinal bands are aggregated to coarser resolutions, such as five- or ten-degree bands, the maximum month-to-month emission variations, in a given year, remain at 25% or less, whereas the average variation is less than 4%.

Table 2. Statistical description of the latitudinal profile of the mass of monthly $FFCO_2$ emissions

		Annual range			Maximum annual range/maximum peak (%)
Year	Maximum peak	Maximum	Average	Standard deviation	
1950	9.49	2.34	0.20	0.40	24.69
1960	12.87	3.51	0.32	0.60	27.29
1970	19.90	3.00	0.42	0.73	15.06
1980	24.25	4.26	0.61	1.06	17.57
1990	26.37	3.54	0.67	0.97	13.43
2000	29.02	5.14	0.78	1.21	17.72

Note: The absolute maximum peak value is given followed by the maximum, average and standard deviation for the annual range in emissions. The annual range was calculated from the maximum and minimum monthly values in each of the 128 non-zero values for emissions in one-degree bands. The standard deviation is larger than the average because the distribution contains a few large values for the annual range. All emissions are reported in Tg C. The final column is a ratio of the third and second columns expressed as a percentage.

Table 3. Statistical description of the longitudinal profile of the mass of monthly $FFCO_2$ emissions

		Annual range			Maximum annual range/maximum peak (%)
Year	Maximum peak	Maximum	Average	Standard deviation	
1950	4.63	1.26	0.09	0.18	27.22
1960	5.34	1.76	0.14	0.25	33.00
1970	8.18	1.46	0.19	0.28	17.90
1980	9.01	1.80	0.26	0.36	20.01
1990	8.91	1.43	0.28	0.34	16.05
2000	10.98	2.16	0.34	0.42	19.65

Note: The absolute maximum peak value is given followed by the maximum, average and standard deviation for the annual range in emissions. The annual range was calculated from the maximum and minimum monthly values in each of the 338–344 (the number varies between years) non-zero values for emissions in one-degree bands. The standard deviation is larger than the average because the distribution contains a few large values for the annual range. All emissions are reported in Tg C. The final column is a ratio of the third and second columns expressed as a percentage.

Table 3 presents some similar basic attributes of the global mass longitudinal profiles. Similar to the latitudinal profiles, the longitudinal profiles indicate that the annual cycle is increasing with time. Although in some longitudinal bands, over a given year, there are some variations in the maximum month-to-month emissions on the order of 35%, the average variation in all one-degree bands is less than 4%. When longitudinal bands are aggregated to coarser resolutions, such as five or ten degrees, the

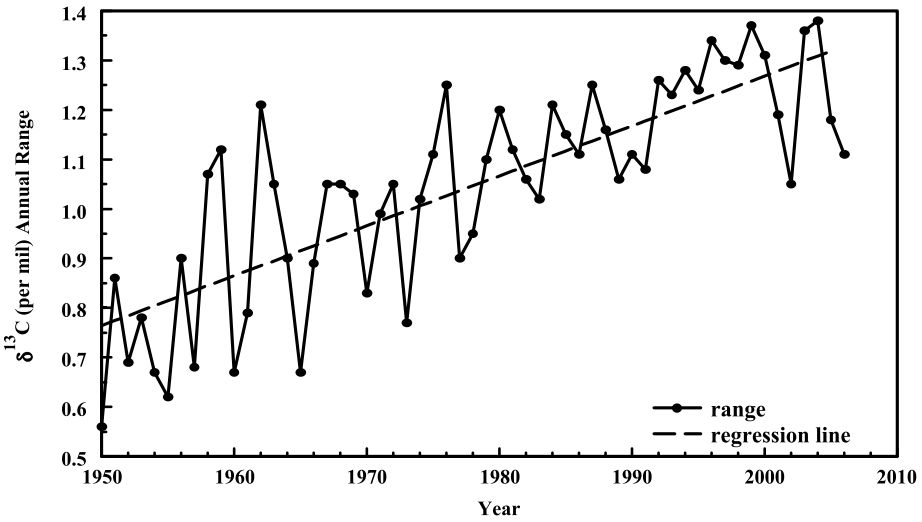

Fig. 10. The annual range in δ^{13}C of $FFCO_2$ emissions. The range was calculated from the maximum and minimum monthly values of δ^{13}C for the calendar year. The dashed line is a linear regression through the annual values.

maximum month-to-month emission variations, in a given year, are 40% or less, whereas the average variation is less than 6%.

To give a visual sense of how the latitudinal and longitudinal profiles change with time, Figs. 4 and 5 plot decadal December emission profiles. A plot of January through December emission profiles for a given year is not shown because of the generally small variation (<0.80 Tg C from Tables 2 and 3) in emissions in any one given year. Figs. 4 and 5 show that the average change in December emissions is 3.58 (latitudinally) and 1.33 (longitudinally) Tg C from 1950 to 2000. These results are in agreement with the findings of Andres et al. (1996), which stated that emissions were generally growing and slowly moving south with time.

Nassar et al. (personal communication, 2010) use the 1950–2006 gridded monthly data (from which Figs. 4 and 5 of this manuscript were created) to help model global atmospheric CO_2 concentrations and transport. Their use of the monthly time series (as compared to use of the annual time series previously available) results in changes of surface $FFCO_2$ concentrations exceeding 1 ppm near high $FFCO_2$ emitting regions (e.g. parts of North America, Europe and Asia). These $FFCO_2$ concentration changes have significant ramifications for results from inverse models.

Data as seen in Tables 2 and 3 and Figs. 4 and 5, and the work of others [e.g. Nassar et al. (personal communication, 2010)] lead to the conclusion that higher temporal resolution $FFCO_2$ data can lead to improved knowledge of the global carbon cycle. For finer geographic scale studies, such as regional or local, finer time scale emissions estimates should be increasingly important—especially when $FFCO_2$ emissions are combined with atmospheric transport models to calculate concentration fields downwind of the emission sources (e.g. at flask or tall tower sampling sites).

3.2. Stable carbon isotope results and discussion

Stable carbon isotopes provide an important constraint to distinguish different components of the carbon cycle and to validate model simulations of the global carbon cycle. $FFCO_2$ emissions show a strong seasonal pattern in their stable carbon isotope signature (Fig. 6). Emissions are generally heavier (less negative values of δ^{13}C) during the Northern Hemisphere summer and generally lighter (more negative values of δ^{13}C) during the Northern Hemisphere winter. Multiple linear regression analysis shows that while the monthly dependence in any given year is strongly correlated to gas consumption, the overall trend (i.e. years 1950–2006) is most strongly correlated to liquid fuel consumption. However, the precipitous drop from 1950 to 1971 is most strongly correlated to increased global consumption of gas. Natural gas is characterized by very low values of δ^{13}C and an increase in gas consumption with respect to solid and liquid fuels is observed (as expected) to be accompanied by a drop in the mean of δ^{13}C signature of emissions.

With time, the amplitude of the annual range in δ^{13}C in annual emissions is increasing, although not in a monotonic, linear fashion (Fig. 10). This increase echoes similar results seen in atmospheric flask samples and in situ monitoring networks (e.g. Keeling et al., 2005). Multiple linear regression analysis shows that no single component correlates strongly to this increase with amplitude over time; solid, liquid, gas and cement all have similar correlation coefficients (0.71–0.77) whether one looks at the entire 1950–2006 time series or the 1950–1971 subset (0.43–0.50).

Table 4 presents some basic attributes of the global latitudinal δ^{13}C profiles. Although in some latitudinal bands, over a given year, there are some variations in the month-to-month emissions on the order of 7%, the average variation for all one-degree

Table 4. Statistical description of the latitudinal profile of the $\delta^{13}C$ signature of monthly $FFCO_2$ emissions

		Annual range			Maximum annual range/minimum peak (%)
Year	Minimum peak	Maximum	Average	Standard deviation	
1950	−35.09	1.26	0.33	0.37	−3.60
1960	−34.12	1.38	0.40	0.37	−4.03
1970	−33.61	1.30	0.48	0.42	−3.87
1980	−31.98	1.98	0.69	0.56	−6.20
1990	−34.16	1.90	0.80	0.57	−5.56
2000	−36.34	2.44	0.94	0.66	−6.72

Note: The minimum peak value is given followed by the maximum, average and standard deviation for the annual range in emissions. The annual range was calculated from the maximum and minimum monthly values in each of the 128 non-zero values for emissions in one-degree bands. All emissions are reported in per mil. The final column is a ratio of the third and second columns expressed as a percentage.

Table 5. Statistical description of the longitudinal profile of the $\delta^{13}C$ signature of monthly $FFCO_2$ emissions

		Annual range			Maximum annual range/minimum peak (%)
Year	Minimum peak	Maximum	Average	Standard deviation	
1950	−33.30	1.36	0.44	0.46	−4.08
1960	−34.16	1.52	0.65	0.49	−4.45
1970	−34.89	2.24	0.85	0.51	−6.42
1980	−35.22	3.08	1.20	0.83	−8.75
1990	−36.16	2.85	1.22	0.73	−7.88
2000	−37.45	5.38	1.35	0.87	−14.37

Note: The minimum peak value is given followed by the maximum, average and standard deviation for the annual range in emissions. The annual range was calculated from the maximum and minimum monthly values in each of the 343–344 non-zero values for emissions in one-degree bands (the number of non-zero mass emission one degree bands is different than that in Table 3 because some bands have the same mass but are composed of different fuels with different $\delta^{13}C$ signatures). All emissions are reported in per mil. The final column is a ratio of the third and second columns expressed as a percentage.

bands is less than 3%. When latitudinal bands are aggregated to coarser resolutions, such as five or ten degrees, the month-to-month emission variations, in a given year, are 6% or less, whereas the average variation is less than 3%.

Table 5 presents some basic attributes of the global longitudinal $\delta^{13}C$ profiles. Although in some longitudinal bands, over a given year, there are some variations in the month-to-month emissions on the order of 14%, the average variation for all one degree bands is less than 4%. When longitudinal bands are aggregated to coarser resolutions, such as five or ten degrees, the month-to-month emission variations, in a given year, are 10% or less, whereas the average variation is less than 4%. Tables 4 and 5 also capture the increasing amplitude of the annual cycle over time.

To give a visual sense of how the latitudinal and longitudinal $\delta^{13}C$ profiles change with time, Figs. 7 and 8 plot decadal December emission profiles. A plot of January through December emission profiles for a given year is not shown because of the generally small variation (<1.40 per mil from Tables 4 and 5) in emissions in any one given year. Figures 7 and 8 show that the average change in December emissions is 6.60 (latitudinally) and 5.14 (longitudinally) per mil from 1950 to 2000.

Data as seen in Tables 4 and 5 and Figs. 7 and 8 lead to the conclusion that increasing temporal resolution for $FFCO_2$ emissions from annual to finer time scales may become even more important for global carbon cycle studies when the $\delta^{13}C$ signature of those emissions is considered. The average signatures seen in Tables 4 and 5 are easily measurable and differentiated by modern day analytical techniques. However, full utilization of the insights that $\delta^{13}C$ signatures could provide will only be realized when $\delta^{13}C$ measurements become more common and a better understanding of the magnitude and range of biologic processes on $\delta^{13}C$ signatures is more fully understood.

3.3. *Establishment of a statistically robust seasonal cycle in* $FFCO_2$ *emissions*

Given these descriptions of the monthly, global pattern of $FFCO_2$ emissions, are the estimated distributions significantly different statistically from a default distribution throughout the year (i.e. that 1/12 of annual emissions occurs in each month)? Figure 11 conclusively shows that the answer to this question is the affirmative. Figure 11 plots the average of 57 years of monthly distributions and their spread over two standard deviations. Data have been plotted in units of monthly fractions instead of absolute mass to ease comparisons. It is clear that the vast majority of months are statistically different from a uniform distribution at one, two or three standard deviations.

3.4. *Calendar versus statistical months*

Is the statistically significant conclusion of Fig. 11 affected by the use of actual calendar months instead of equally sized mathematical months over the course of a given year? The choice was made to use calendar months in this analysis because the basic raw data to construct the monthly fractions are reported in actual calendar months, not mathematical months. Also, the modelling community itself is undecided which to use: some modellers use actual calendar months whereas others use mathematical months. Reconstructing Fig. 11 with mathematical months (reconstruction not shown, but the figure is similar to Fig. 11 except the emissions in February are similar to those in January) reveals all mathematical months are statistically different from the uniform 1/12 distribution at one and two standard deviations. At

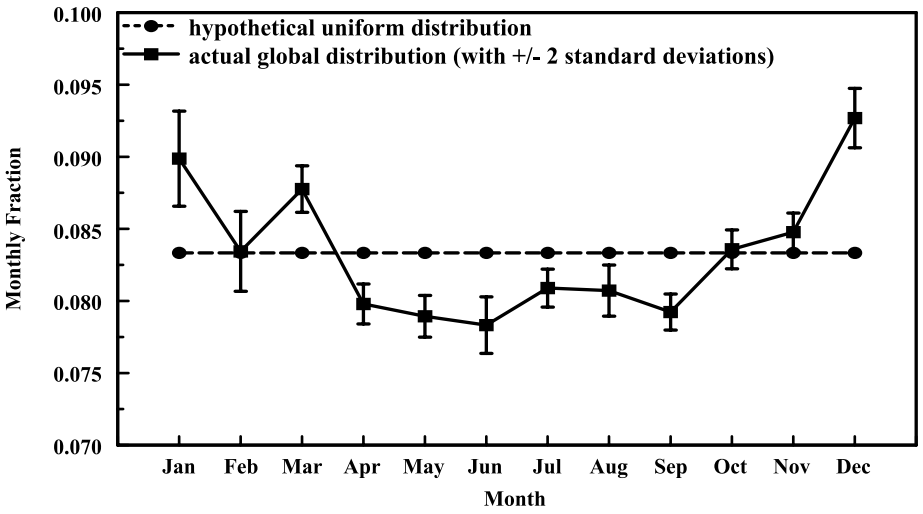

Fig. 11. Comparison of actual global monthly fractions with a hypothetical uniform distribution. Monthly fractions were calculated from solid, liquid and gas fuels, gas flaring and cement production for 57 years (1950–2007). At one and two standard deviations, 10 of 12 months are statistically significantly different from the uniform distribution (equal to 0.083). At three standard deviations (not shown), eight of 12 months remain statistically significantly different from the uniform distribution.

three standard deviations, 10 of 12 months are statistically different from the uniform distribution.

4. Uncertainties

Constructing a global data set on $FFCO_2$ emissions on a monthly basis from actual data (i.e. going from Figs. 2 and 3) is possible, but requires pushing very hard on the data that can be assembled. There are three basic assumptions in the proportional-proxy method used here: (1) the proportional method faithfully reproduces the emission pattern for a given fuel in a given country, (2) the proxy method is applicable when the monthly pattern from a known country is applied to that same country for years when no monthly data exist and (3) the proxy method is applicable when the monthly pattern from a known country is applied to a different country. These assumptions are superimposed on recognition that global $FFCO_2$ emissions are dominated by a small number of countries and that there is some real monthly data on at least some emissions during recent years. Each of the three assumptions is examined here.

4.1. Does the proportional method work?

The validity of the proportional method has been explored in Gregg and Andres (2008). The basic conclusion from this work was that similar results are obtained from the proportional methodology and from more detailed, bottom-up, accounting methodologies. The accuracy of the method can be assessed for countries where detailed bottom-up inventories and the proportional method have both been used. This assessment has been done for the United States where the differences in monthly national emission estimates were found to be less than 2% (Gregg and Andres, 2008). We expect similar results for other countries, but realize that the high degree of success in the United States was due to the large fraction of the total fuel consumption that was incorporated into the proportional method: 87%, 86%, 92% and 88% for solid, liquid and gas fuels, and for the three fuels combined (mass-emissions weighted), respectively. For the 20 other countries to which the proportional method was applied, similar amounts of the total fuel stream (e.g. 70–90%) were accounted by monthly data input to the proportional method. The worst coverage was for Brazilian gas fuels where only 22% of the fuel stream was covered by monthly data. Overall, the mass-emissions weighted, three-fuels-combined percentage for all countries was 86%. We estimate the error for the proportional method, on a global basis, is 5% to account for the varying levels of fractional fuel coverage.

4.2. Does the proxy method work internally?

The validity of the proxy method centres on whether the proxy monthly fraction pattern is a faithful representation of the actual monthly fraction pattern. Available research time, financial cost and the actual existence of monthly data for each country limited the collection of monthly data for all countries and for all years.

The case of applying a proxy monthly fraction pattern from one country to that same country for years in which the monthly fraction pattern is unknown is tested by examining the standard deviation of the monthly fraction pattern. Because all known monthly fraction patterns are initially used, the test removes one monthly fraction pattern from the set of known monthly fraction patterns for a given country and fuel, calculates the standard deviation of the remaining monthly fraction patterns and then tests the removed monthly fraction pattern to determine if it

Table 6. Test results of using a known monthly fraction pattern from a country for that same country for a year with an unknown monthly fraction pattern

Fuel	No. of years (all data)	Testable years (no. of years ≥4)	Testable months (no. of years ≥4)	Percent of months >±1 *SD*	>±2 *SD*	>±3 *SD*
Solid	335	334	4008	34.4	8.4	2.2
Liquid	447	444	5328	31.1	7.6	2.3
Gas	357	348	4176	32.9	7.7	2.3

Note: Testable years are the subsets of all years for countries with fuel time series longer than 4 years. Testable months are related to years by a factor of 12. The last three columns show the percentage of testable months outside defined standard deviation limits. For a normal distribution, the percent of data greater than one, two or three standard deviations is 31.7%, 4.6% and 0.3%, respectively.

resides within the average plus or minus one, two or three standard deviations. The test was completed for all 1126 monthly fraction pattern time series (Table 6). The test revealed that the data are near normally distributed. Thus, the use of a monthly pattern from a known year for a given country and fuel is a reasonable approximation of the monthly pattern from an unknown year for that same country and fuel. In addition, graphs (not shown) of the monthly data used to construct Table 6 display no particular months that are unduly abnormal (i.e. the monthly distributions of the number of months greater than one, two or three standard deviations are relatively flat). Therefore, no systematic monthly bias is introduced when using the known monthly distributions for unknown distributions. The error introduced by this approximation (using a known monthly fraction pattern from one country for an unknown pattern for the same country) is 4%, calculated by the mass-emissions-weighted standard deviation. As mentioned earlier, it is important to reiterate here that although the Monte Carlo method used here captures the basic pattern and variability of the annual cycle, it does not preserve any genuine temporal trends in the annual cycle. Therefore, for example, the growth of a secondary maximum (as seen during the summer in the United States) will not be captured unless actual data is used.

The earlier analysis demonstrates that there is a small and quantifiable error introduced by substituting data from any given year for a year with no data over the period extant data. It does not directly address the period prior to when there is monthly data (Figs. 1 and 2). Extending this proxy method back in time is subject to increasing uncertainty as the time increases allowing differences in the spatial and temporal patterns of energy use. Therefore, to accommodate the interest in using the annual distribution of emissions in modelling exercises and the temporal limits of the monthly data, this study has extended the proxy method back to 1950. Extension of this methodology further back in time is not warranted based upon the existing monthly $FFCO_2$ data sets.

4.3. Does the proxy method work externally?

The case of applying a proxy monthly fraction pattern from one country to an unknown country is tested by two methods. First, data do exist for some fuels and for some countries not listed in Table 1. The general lack of data and the small percentage of fuel (relative to global totals) used in these countries are some of the reasons Table 1 was limited to 21 countries. However, this proxy approximation can be tested by comparing the actual country time series to the proxy time series used for that country. This test examines how well the proxy assignment was made. Secondly, this approximation is tested via another Monte Carlo simulation in which the proxy assignments are changed. This test examines how sensitive the global pattern is to the proxy assignments.

4.3.1. Suitable proxy assignment made? Figure 12 shows the results of comparing actual Pakistani gas data with its proxy data based on the pattern of Indian gas data. Although the Pakistani data do not fully imitate the late-year peak of the Indian data, of the 48 Pakistani data points shown, 39 of the data points (81%) fall within the plus or minus one standard deviation shaded area of the Indian proxy. At two standard deviations, 47 data points (98%) fall within the shaded area (not shown). At three standard deviations, all of the Pakistani data fall within the shaded area (not shown). In addition to the magnitude of the actual Pakistani data falling within one standard deviation of the India gas data proxy, the phasing of peaks and troughs have some consistency between the two data sets.

Figure 13 shows the results of comparing actual Belgian gas data with its proxy data based on the pattern of French gas data. Of the 36 Belgian data points shown, 11 points (31%) fall within the plus or minus one standard deviation shaded area of the French proxy. At two standard deviations, 20 data points (56%) fall within the shaded area (not shown). At three standard deviations, 24 data points (67%) fall within the shaded area (not shown). The small standard deviation of the French proxy highlights well the consistency of the actual Belgian data with the phasing of proxy peaks and troughs. The actual Belgian data has a smaller seasonal amplitude than the French proxy.

Another useful comparison can be made by comparing the annual cycle of total (i.e. solid+liquid+gas+gas flaring+cement) $FFCO_2$ emissions derived here with totally independent data sets from other sources. For example, our estimate of the annual cycle for The Netherlands is based on a proxy from German

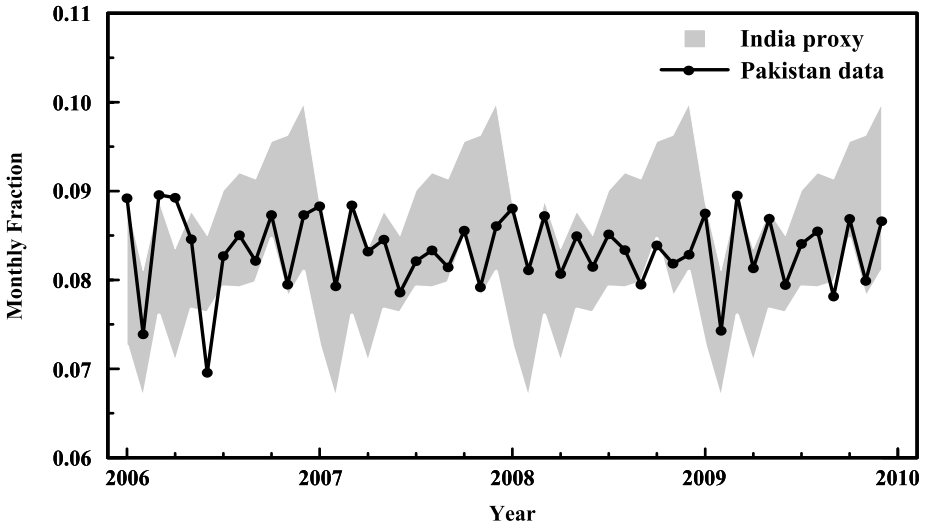

Fig. 12. Comparison of Indian proxy and actual Pakistani gas data. The Indian proxy is represented by a shaded area, showing the average plus or minus one standard deviation. The Indian pattern repeats itself for 4 years as any of the 35 years of actual Indian data may be chosen by the Monte Carlo simulation to represent the monthly pattern for a particular Pakistani year. The Pakistani gas data are for Pakistan gas production. Because Pakistani imports, exports, changes in stock and gas flaring are relatively small (less than 4% of production in year 2006), the national production data shown mirror closely the national gas consumption data. Pakistani gas data were taken from Progress (2006–2009).

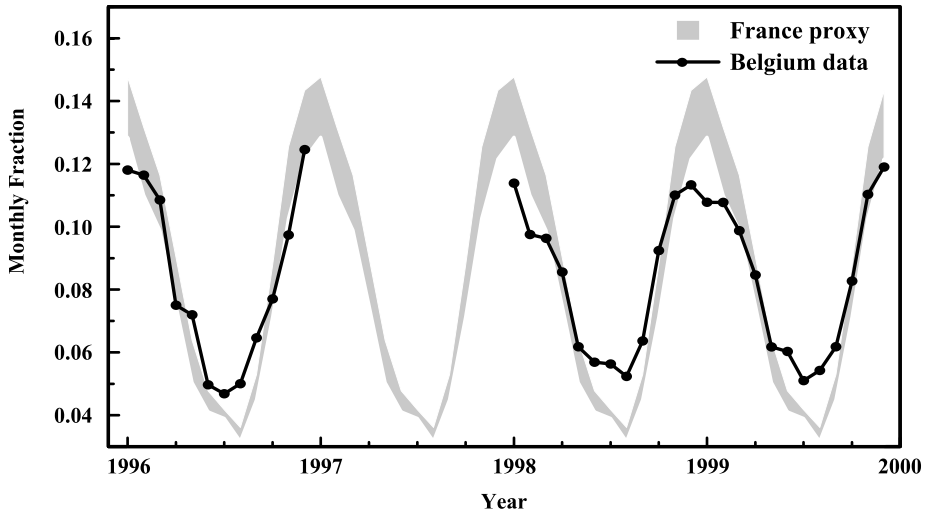

Fig. 13. Comparison of French proxy and actual Belgian gas data. The French proxy is represented by a shaded area, showing the average plus or minus one standard deviation. The French pattern repeats itself for 4 years as any of the 19 years of actual French data may be chosen by the Monte Carlo simulation to represent the monthly pattern for a particular Belgian year. The Belgian gas data are for Belgium gas sales and/or consumption (the time series contains both). Belgium gas data were taken from Bulletin d'information FIGAZ/A.R.G.B. (1996–2000).

data and there is an independent estimate based on ^{222}Radon data as modelled by van der Laan et al. (2010). A more complete comparison would include back trajectory analysis of the actual air masses sampled by van der Laan et al. and thus the relative contributions of $FFCO_2$ from multiple countries and this more complete analysis would also better harmonize the sampling frequency discrepancies between van der Laan et al. (i.e. bi-weekly) and the data presented here (i.e. monthly). But, the $FFCO_2$ emissions modelled by van der Laan et al. have been directly compared to those from The Netherlands as presented here and the comparison shows qualitative agreement (graph not shown). Both data sets capture the general shape of the annual cycle, although the phasing of the peak in emissions is a bit earlier in the monthly data set presented here. The amplitudes of the two data sets are not identical, nor are they expected to be. Before converting to monthly fractions, the van der Laan et al. data are in units of mass per area and the data presented here are in mass units. Likely the area sampled by van der Laan et al. are not constant with time nor equal to the extent of The Netherlands only.

Obviously, these three examples do not address all 222 proxy assignments (this number is greater than the values in Table 1 because some countries divide or merge over the 1950–2006 time series and Table 1 is for one particular year in that time series). For most of these assignments, monthly fuel consumption data do not exist. However, these examples do give a sense that the phasing of the assignments is close. The magnitude of the assignments may not always be perfect. However, at the global scale, having the correct magnitude is of most importance for the largest emitters since they weight the global pattern the most. Having at least some data on the 21 countries of Table 1 ensures that the weighting factors are generally accurate.

4.3.2. Sensitivity of the global pattern to proxy assignments. The next step to evaluate uncertainty was to run a second Monte Carlo simulation to test how sensitive the global pattern was to the proxy assignments (i.e. a change in weighting assignments). For this final evaluation, the set of Monte Carlo simulations consisted of three tests. In each test, the proxy country assigned to a country with unknown monthly distribution was changed. The first test focused on the Southern Hemisphere, which contains only two countries from among the 21 countries in Table 1. Countries originally assigned to a South African proxy were switched to an Australian proxy and countries originally assigned to an Australian proxy were switched to a South African proxy. The second test added the five proxy equatorial countries from Table 1 to the countries switched. Similar to the Southern Hemisphere test, countries originally assigned to one equatorial country proxy were assigned to another equatorial country proxy. The third test added the remaining proxy Northern Hemisphere countries from Table 1 to the countries switched. Countries originally assigned to one Northern Hemisphere country proxy were assigned to another Northern Hemisphere country proxy. This final test included all of the countries and 20% of global emissions not specifically identified in Table 1. In all three tests, the switching of proxy countries resulted in essentially identical monthly fractions to those already plotted in Fig. 11. This test only switched proxy countries among countries within three broadly similar latitudinal bands; thus, keeping the phasing of seasonality relatively similar and ignoring differences in economies. This test shows that the final global results are relatively insensitive to the exact proxy assignment. Of course, local results will depend heavily on the exact proxy country chosen and the differences between the two results will be directly proportional to the differences between the monthly fractions of the two proxy countries.

Calculating an estimate of the error introduced into the resulting global distribution for the third assumption considers both sets of comparisons performed above: the direct comparison of actual country data with the proxy data and the Monte Carlo simulations. The lack of suitable data sets for direct comparison is troubling, but that lack of data was the motivation for completing this study in the first place: to gain a better understanding of the global, annual cycle of $FFCO_2$ emissions. The Monte Carlo simulations indicate that the global, annual cycle is relatively insensitive to the proxy assignments. We conclude that there is a 4% uncertainty in global monthly emissions as a result of using proxy data for estimating the annual cycle of emissions in other countries, but realize that this error assessment itself is not well constrained.

4.4. Additional uncertainty introduced by the proportional-proxy method

The uncertainty analysis can now be completed for the basic mass data presented in this paper. Realizing that the error for the entire data set is a combination of assumption 1 error (5%) and assumption 2 error (4%) or assumption 1 error and assumption 3 error (4%), the overall error for estimates of the monthly fraction of the total $FFCO_2$ emissions is calculated by the square root of the sum of the squares for either combination. This results in a one sigma error of 6.4%.

4.5. Other uncertainties

Additional uncertainty can also be found in the other data products discussed in this paper. For uncertainties related to the one degree distribution of the global mass of $FFCO_2$ emissions, see Andres et al. (1996). For uncertainties related to the stable isotope signatures, see Andres et al. (2000).

5. Conclusions

This project was initiated in response to many inquiries to CDIAC for $FFCO_2$ emissions estimates at temporal scales finer than 1 year. Survey data on consumption of fossil fuels are broadly available only at annual resolution, but many countries have at least some data on fuel use at monthly resolution. Although these monthly time series are not easily available for many countries and are often short in duration and/or cover only some fuels, there are enough data for enough countries and fuels to assemble a reasonable monthly time series of $FFCO_2$ emissions estimates. This paper documents the data that were available, the extent to which they were manipulated to estimate a global data set, and the limitations of the final data set. The monthly data set has also been displayed spatially over the Earth. Finally, the monthly data set has been described over the same temporal and spatial resolutions in terms of its stable carbon isotopic signature. These monthly data sets are currently being used in several studies including forward and inverse modelling in support of satellite CO_2 retrievals (e.g. Nassar, personal communication, 2010), atmospheric inverse modelling to determine regional carbon sources and sinks (Patra, personal communication, 2009), and atmospheric inverse modelling to determine global carbon sources and sinks in preparation for the IPCC Fifth Assessment Report (V. Brovkin, P. Cadule, M. Cuntz, P. Friedlingstein, J. John, C. Jones, T. Raddatz, personal

communications, 2009, 2010). Monthly data from this study will be available from the Carbon Dioxide Information Analysis Center (CDIAC) website: http://cdiac.esd.ornl.gov/.

This study utilized the best available statistical data available from the 21 largest $FFCO_2$ emitting countries and a proportional-proxy methodology to extend the utility of that data to the globe and to a longer time series. With present national statistical efforts, this approach is pushing against its temporal and spatial limits. If finer temporal and spatial scale data sets are needed by the broader community, then those data sets will need to be created by modelling efforts such as those cited in the introduction to this paper. Alternatively, as called for by others (e.g. NRC, 2010), improvement in the capabilities of national statistical offices/agencies would allow for continuation and improvement of the proportional-proxy method used here. Such support would allow for continuation of exiting relevant time series or creation of new time series used in the proxy portion of this methodology. This support would not only improve the results as obtained herein, but also improve our overall understanding of the carbon cycle in countries receiving such support.

The monthly time series presented here offer promise of increased knowledge about the global carbon cycle. The creation of monthly mass and stable carbon isotopic signature $FFCO_2$ data sets provide new inputs to existing and planned studies of the global carbon cycle. The mass and/or the $\delta^{13}C$ time series should be particularly useful in regional and/or local studies and further modelling efforts should help elucidate the necessary temporal scales for $FFCO_2$ emission time series in relation to pressing carbon cycle study questions.

Finally, this study has increased understanding of the subannual distribution of $FFCO_2$ emissions. For example, when Figs. 3 and 6 are combined with an understanding of the uncertainties of this data set, this study shows that the opposition of seasons between Northern and Southern Hemispheres is not offset by the disparity between the consumption of fossil fuels in Northern and Southern Hemispheres. Thus, Fig. 11 shows a real variation in $FFCO_2$ emissions over the year.

6. Acknowledgments

This work was initially supported by U.S. Department of Energy grant DE-FG02-03ER46030. This work was also sponsored by U.S. Department of Energy, Office of Science, Biological and Environmental Research (BER) programs and performed at Oak Ridge National Laboratory (ORNL). ORNL is managed by UT-Battelle, LLC, for the U.S. Department of Energy under contract DE-AC05-00OR22725. The submitted paper has been authored by a contractor of the U.S. Government under contract DE-AC05-00OR22725. Accordingly, the U.S. Government retains a nonexclusive, royalty-free license to publish or reproduce the published form of this contribution, or allow others to do so, for U.S. Government purposes.

References

Andres, R. J., Marland, G., Fung, I. and Matthews, E. 1996. A one degree by one degree distribution of carbon dioxide emissions from fossil fuel consumption and cement manufacture, 1950–1990. *Global Biogeochem. Cycles* **10**, 419–429.

Andres, R. J., Fielding, D. J., Marland, G., Boden, T. A., Kumar, N., and co-authors. 1999. Carbon dioxide emissions from fossil-fuel use, 1751–1950. *Tellus* **51B**, 759–765.

Andres, R. J., Marland, G., Boden, T. and Bischof, S. 2000. Carbon dioxide emissions from fossil fuel consumption and cement manufacture, 1751–1991, and an estimate of their isotopic composition and latitudinal distribution. In: The Carbon Cycle. Wigley, T. M. L. and Schimel, D. S. (eds.). Cambridge University Press, Cambridge, 53–62.

Blasing, T. J., Broniak, C. and Marland. G. 2005. The annual cycle of fossil-fuel carbon dioxide emissions in the United States. *Tellus*, **57B**, 107–115.

Boden, T. A., Marland, G. and Andres, R. J. 2009. Global, regional, and national fossil-fuel CO_2 emissions. Carbon Dioxide Information Analysis Center, Oak Ridge National Laboratory, U.S. Department of Energy, Oak Ridge, TN, USA, doi:10.3334/CDIAC/00001.

British Petroleum (BP). 2009. Statistical review of world energy, London. Available at: http://www.bp.com/productlanding.do?categoryId=6848&contentId=7033471. Accessed 5 Aug 2009.

Bulletin d'information FIGAZ/A.R.G.B. monthly issues 1996–2000. Brussels.

Ciais, P., Tans, P. P., White, J. W. C., Trolier, M, Francey, R. J., and co-authors. 1995. Partitioning of ocean and land uptake of CO_2 as inferred by $\delta^{13}C$ measurements from the NOAA Climate Monitoring and Diagnostics Laboratory global air sampling network. *J. Geophys. Res*. **100**, 5051–5070.

Corbin, K. D., Denning, A. S. and Gurney, K. R. 2010. The space and time impacts on U.S. regional atmospheric CO_2 concentrations from a high resolution fossil fuel CO_2 emissions inventory. *Tellus* **62B**, 506–511, doi:10.1111/j.1600-0889.2010.00480.x.

Denman, K. L., Brasseur, G., Chidthaisong, A., Ciais, P., Cox, P. M., Dickinson, R. E., and co-authors. 2007. Couplings between changes in the climate system and biogeochemistry. In: *Climate Change 2007: The Physical Science Basis. Contribution of Working Group I to the Fourth Assessment Report of the Intergovernmental Panel on Climate Change* (eds. Solomon, S., Qin, D., Manning, M., Chen, Z., Marquis, M., and co-editors). Cambridge University Press, Cambridge, UK and New York, NY, USA, 516, 517.

Energy Information Administration (EIA). 2010. International energy statistics. Available at: http://tonto.eia.doe.gov/cfapps/ipdbproject/IEDIndex3.cfm?tid=90&pid=44&aid=8. Accessed 5 Aug 2009.

Etemad, B., Luciani, J., Bairoch, P. and Toutain, J.-C. 1991. *World Energy Production 1800–1985*. Librarie DROZ, Geneva, Switzerland.

European Union (EU). 2009. Directive 2003/87/EC of the European Parliament and of the Council of 13 October 2003 Establishing a Scheme for Greenhouse Gas Emission Allowance Trading Within the Community and Amending Council Directive 96/61/EC. http://eur-lex.europa.eu/LexUriServ/LexUriServ.do?uri=CONSLEG:2003L0087:20090625:EN:PDF.

Forster, P., Ramaswamy, V., Artaxo, P., Berntsen, T., Betts, R., and co-authors. 2007. Changes in atmospheric constituents and in

radiative forcing. In: *Climate Change 2007: The Physical Science Basis. Contribution of Working Group I to the Fourth Assessment Report of the Intergovernmental Panel on Climate Change* (eds. Solomon, S., Qin, D., Manning, M., Chen, Z., Marquis, M., and co-editors). Cambridge University Press, Cambridge, UK and New York, NY, USA, 138.

Gregg, J. S. and Andres, R. J. 2008. A method for estimating the temporal and spatial patterns of carbon dioxide emissions from national fossil-fuel consumption. *Tellus* **60B**, 1–10, doi:10.1111/j.1600-0889.2007.00319.x.

Gregg, J. S., Andres, R. J. and Marland, G. 2008. China: emissions pattern of the world leader in CO_2 emissions from fossil fuel consumption and cement production. *Geophys. Res. Lett.* **35**, L08806, doi:10.1029/2007GL032887.

Gregg, J. S., Losey, L. M., Andres, R. J., Blasing, T. J. and Marland, G. 2009. The temporal and spatial distribution of carbon dioxide emissions from fossil-fuel use in North America. *J. Appl. Meteorol. Climatol.* **48**, 2528–2542, doi:10.1175/2009JAMC2115.1.

Gurney, K. R., Chen, Y. H., Maki, T., Kawa, S. R., Andrews, A., and co-authors. 2005. Sensitivity of atmospheric CO_2 inversions to seasonal and interannual variations in fossil fuel emissions, *J. Geophys. Res.*, **110**, D10308, doi:10.1029/2004JD005373.

Gurney, K. R., Mendoza, D. L., Zhou, Y., Fischer, M. L., Miller, C. C., and co-authors. 2009. High resolution fossil fuel combustion CO_2 emission fluxes for the United States. *Environ. Sci. Technol.* **43**, 5535–5541.

Intergovernmental Panel on Climate Change (IPCC). 2006. In: *2006 IPCC Guidelines for National Greenhouse Gas Inventories* (eds. Eggleston, H. S., Buendia, L., Miwa, K., Ngara, T. and Tanabe, K.). Institute for Global Environmental Strategies, Hayama, Japan.

IPCC. 2010. In: *Expert Meeting on Uncertainty and Validation of Emissions Inventories* (eds. Eggleston, H. S., Baasansuren, J., Tanabe, K., Srivastava, N.), Institute for Global environmental Strategies, Hayama, Japan, 26.

International Energy Agency. 2009. *World Energy Statistics 2009*. International Energy Agency, Paris.

Keeling, R. F., Najjar, R. P., Bender, M. L. and Tans, P. P. 1993. What atmospheric oxygen measurements can tell us about the global carbon cycle. *Global Biogeochem. Cycles* **7**, 37–67.

Keeling, C. D., Chin, J. F. S. and Whorf, T. P. 1996. Increased activity of northern vegetation inferred from atmospheric CO_2 measurements. *Nature* **382**, 146–149.

Keeling, C. D., Piper, S. C., Bacastow, R. B., Wahlen, M., Whorf, T. P., and co-authors. 2005. Atmospheric CO_2 and $^{13}CO_2$ exchange with the terrestrial biosphere and oceans from 1978 to 2000: observations and carbon cycle implications. In: *A History of Atmospheric CO_2 and Its Effects on Plants, Animals, and Ecosystems* (eds. Ehleringer, J. R., Cerling, T. E. and Dearing, M. D.). Springer Verlag, New York, 83–113.

Le Quere, C., Raupach, M. R., Canadell, J. G., Marland, G., Bopp, L., and co-authors. 2009. Trends in the sources and sinks of carbon dioxide. *Nat. Geosci.* **2**, 831–836, doi:10.1038/ngeo689.

Levin, I., Naegler, T., Kromer, B., Diehl, M., Francey, R. J., and co-authors. 2010. Observations and modelling of the global distribution and long-term trend of atmospheric $^{14}CO_2$. *Tellus* **62** *B*, doi:10.1111/j.1600-0889.2009.00446.x.

Losey, L. M., Andres, R. J. and Marland, G. 2006. Monthly estimates of carbon dioxide emissions from fossil-fuel consumption in Brazil during the late 1990s and early 2000s. *Area* **38**, 445–452, doi:10.1111/j.1475-4762.2006.00713.x.

Macknick, J. 2009. *Energy and Carbon Dioxide Emission Data Uncertainties. IR-09-032. International Institute for Applied Systems Analysis*, Laxenburg, Austria, 55.

Marland, G. and Rotty, R. M. 1984. Carbon dioxide emissions from fossil fuels: a procedure for estimation and results for 1950–1982. *Tellus* **36B**, 232–261.

National Research Council (NRC). 2010. *Verifying Greenhouse Gas Emissions: Methods to Support International Climate Agreements*. The National Academies Press, Washington, DC, 124.

New York City (NYC). 2010. Greenhouse gas emission inventory. Available at: http://www.nyc.gov/html/planyc2030/html/emissions/emissions.shtml. Accessed 6 May 2010.

Oda, T. and Maksyutov, S. 2011. A very high resolution (1 km $\times$ 1 km) global fossil fuel CO_2 emission inventory derived using a point source database and satellite observations of nighttime lights. *Atmos. Chem. Phys.* **11**, 543–556, doi:10.5194/acp-11-543-2011.

Olivier, J. G. J., Van Aardenne, J. A., Dentener, F., Pagliari, V., Ganzeveld, L. N. and co-authors. 2005. Recent trends in global greenhouse gas emissions: regional trends 1970–2000 and spatial distribution of key sources in 2000. *Environ. Sci.* **2**, 81–99, doi:10.1080/15693430500400345.

Pregger, T., Scholz, Y. and Friedrich, R. 2007. Documentation of the anthropogenic GHG emission data for Europe provided in the frame of CarboEurope GHG and CarboEurope IP. Final Report. Institute of Energy Economics and the Rational Use of Energy, University of Stuttgart.

Progress. monthly issues. 2006–2009. Pakistan Petroleum Limited, Karachi.

Rayner, P. J., Raupach, M. R., Paget, M., Peylin, P. and Koffi, E. 2010. A new global gridded dataset of CO_2 emissions from fossil fuel combustion: Methodology and evaluation. *J. Geophys. Res.* **115**, D19306, doi:10.1029/2009JD013439.

Thoning, K. W., Tans, P. P. and Komhyr, W. D. 1989. Atmospheric carbon dioxide at Mauna Loa Observatory 2. Analysis of the NOAA GMCC data, 1974–1985. *J. Geophys. Res.* **94**, 8549–8565.

United Nations. 1992. United Nations framework convention on climate change. Available at: http://unfccc.int. Accessed 21 Apr 2010.

United Nations. 1998. Kyoto protocol to the United Nations framework convention on climate change. Available at: http://unfccc.int. Accessed 21 Apr 2010.

United Nations. 2008. *2006 Energy Statistics Yearbook*. Statistics Division, United Nations Department for Economic and Social Information and Policy Analysis, New York.

Van Der Laan, S., Karstens, U., Neubert, R. E. M., van der Laan-Luijkx, I. T. and Meijer, H. A. J. 2010. Observation-based estimates of fossil fuel-derived CO_2 emissions in the Netherlands using $\Delta^{14}C$, CO and ^{222}Radon. *Tellus* **62B**, 389–402, doi:10.1111/j.1600-0889.2010.00493.x.

Supporting Information

Additional Supporting Information may be found in the online version of this article:

Appendix S1. Individual country monthly data sources

Appendix S2. Proxy country mapping table

Please note: Wiley-Blackwell is not responsible for the content or functionality of any supporting materials supplied by the authors. Any queries (other than missing material) should be directed to the corresponding author for the article.